JOURNAL OF Applied Polymer SCIENCE

Anion Exchange Membranes Derived from Nafion Precursor for the Alkaline Fuel Cell: Effect of Cation Type on Properties

Holly L. S. Salerno, Yossef A. Elabd
Department of Chemical and Biological Engineering, Drexel University, Philadelphia, Pennsylvania 19104
Correspondence to: Y. A. Elabd (E-mail: elabd@drexel.edu)

ABSTRACT: Highly stable hydroxide conducting membranes are necessary for solid-state alkaline fuel cells to have long performance lifetimes. In this study, we used solid-state chemistry to synthesize Nafion-based anion exchange membranes (AEMs) with a variety of covalently attached cations, including trimethylammonium, trimethylphosphonium, piperazinium, pyrrolidinium, pyridinium, and quaternized 1,4-diazabicyclo[2.2.2]octane. Infrared spectroscopy confirms a partial asymmetric functionalization of all cations with the exception of pyridinium. The AEMs that were successfully synthesized all exhibited sufficient water uptake and conductivity. The effect of cation type on AEM chemical and thermal stability was investigated as a function of various conditions (e.g., hydration levels, temperature, and pH). High chemical and thermal stability was observed for all successfully synthesized AEMs with the exception of the trimethylphosphonium cation AEM. © 2012 Wiley Periodicals, Inc. J. Appl. Polym. Sci. 000: 000–000, 2012

KEYWORDS: ion-containing polymers; membranes; fuel cells; conductivity; ion exchange

Received 1 December 2011; accepted 13 April 2012; published online
DOI: 10.1002/app.37874

INTRODUCTION

Alkaline fuel cells (AFCs) have the potential to be substantially less expensive than their proton exchange membrane fuel cell counterparts due to more facial electrode kinetics in basic environments making the use of nonprecious metal catalysts possible.[1–3] However, traditional AFCs did not transition to wide-scale commercial use due to the limitations of the liquid potassium hydroxide (KOH) electrolyte, specifically due to its carbon dioxide (CO_2) sensitivity. When CO_2 is present in the fuel, it can react with hydroxide ions to form both bicarbonate (HCO_3^-) and carbonate (CO_3^{2-}) anions, which coordinate with the free metal cations (K^+) to produce crystallite precipitates (i.e., $KHCO_3$ and K_2CO_3). Carbonate precipitates reduce catalyst activity, limit fuel mass transfer in the electrode, and reduce electrolyte conductivity, which all lead to a rapid and drastic decrease in fuel cell performance.[1,4] Replacement of the liquid KOH electrolyte with a solid polymer anion exchange membrane (AEM) with covalently tethered cationic groups eliminates the carbonate precipitate problem.[1,5] Therefore, the use of hydroxide conducting AEMs as solid electrolytes has spurred a resurgence of research in AFCs.[1,6]

Traditionally, AEMs have been used as ion exchange resins and separation membranes for electrodialysis.[7–10] AEMs are typically synthesized by covalently attaching onium-class cations (ammonium, phosphonium, and sulfonium) to various polymers. Implementation of AEMs to AFCs is challenging due to the low chemical stability of the onium cationic groups in the presence of high pH environments (e.g., high hydroxide concentrations) at low hydration levels and elevated temperatures.[1,3] Trostyanskaya and Makarova[7] reported that ammonium cations are the most stable, whereas sulfonium cations are the least stable among the onium-class cations.

To date, most hydroxide conducting AEMs synthesized consist of a covalently attached ammonium cation as the conducting group.[11–28] Ammonium cations in AEMs are susceptible to neutralization from hydroxide ion attack via a number of degradation mechanisms, including S_N2, Hofmann (E2) elimination, Stevens rearrangement, and Sommelet–Hauser rearrangement.[3,29–32] Pivovar and coworkers[3,31] studied the decomposition of the small molecule trimethylammonium equivalent, $N^+(CH_3)_4OH^-$, and found that while it is reasonably stable in alkaline media, when the hydroxide ion has less than three water molecules in the hydration shell it activates the degradation of the cation resulting in a neutral nonconductive amine. Several other studies have investigated other cations in AEMs, such as phosphonium, pyridinium, and quaternized 1,4-diazabicyclo[2.2.2]octane (DABCO).[7–10,19,32–52] The chemical stability of these AEMs has varied depending on the chemistry of the side chain (link

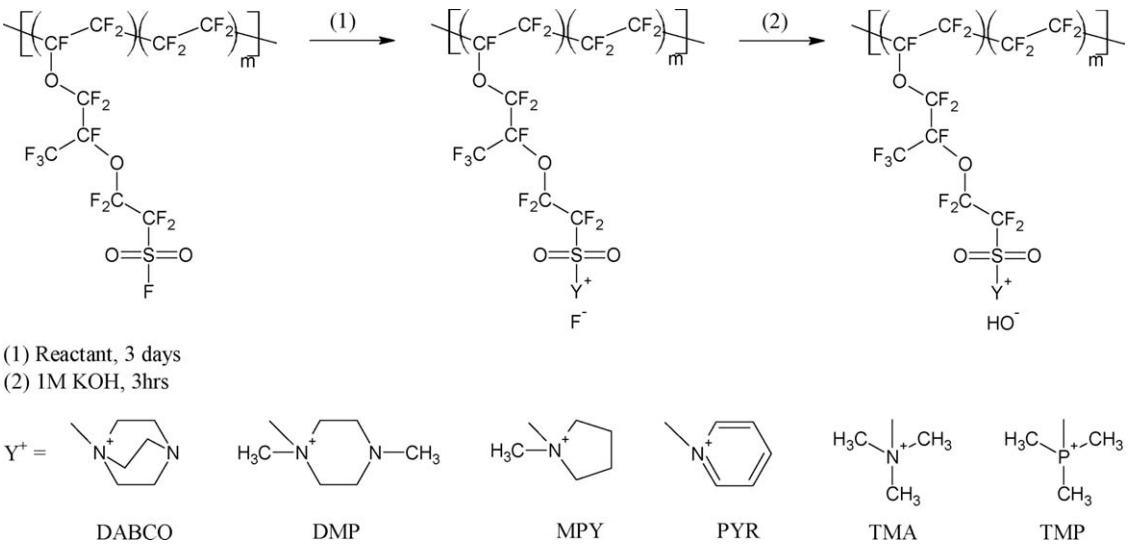

Scheme 1. Synthesis of Nafion-based AEMs with various cations.

between the polymer backbone and cation) and substituent groups around the cation. However, this does not appear to be comprehensive study that compares a wide variety of cations covalently attached to the same polymer with the same side chain. In other words, what is the comparative chemical stability of a cation in an AEM when all other things are equal?

In this study, we investigate the chemistry and chemical stability of Nafion-based AEMs with a variety of covalently attached cations, including ammonium, phosphonium, piperazinium, pyrrolidinium, pyridinium, and quaternized DABCO. Recently, several studies have reported on the functionalization of the Nafion precursor to produce an AEM, that is, reacting the sulfonyl fluoride end group (—SO_2F) to a covalently attached cation (—SO_2X^+).[53–56] However, to date, little is known about Nafion-based AEMs and without a clear understanding of the chemical stability of hydroxide conducting AEMs as a function of cation type it will be difficult to design an AEM for long-lasting AFC performance. In this study, infrared spectroscopy confirms the successful synthesis of AEMs with all of these cations with the exception of pyridinium, whereas high chemical and thermal stability was demonstrated for all these successfully synthesized AEMs with the exception of the phosphonium AEM.

EXPERIMENTAL

Materials

DABCO (98%), 1,4-dimethylpiperazine (DMP, 98%), 1-methylpyrrolidine (MPY, ≥ 99%), pyridine (PYR, 99.8%, anhydrous), trimethylamine (TMA, ~45% in water), trimethylphosphine (TMP, 1*M* in toluene) KOH, (ACS reagent, >85%), potassium chloride (KCl, Sigma Ultra, 99.0%), hydrochloric acid (HCl, ACS plus, 37.4%), and dimethylformamide (DMF, 99.8%, anhydrous) were purchased from Sigma-Aldrich, St. Louis, MO and used as received. Ultrapure deionized (DI) water (resistivity > 16 MΩ cm) was used. Commercially extruded Nafion precursor film was purchased from Ion Power, Inc., New Castle, DE [Nafion 111P, 1100 EW, ~25 μm (0.001 in) dry thickness] and was used as received.

Synthesis of Nafion-Based Anion Exchange Membranes

Nafion-based AEMs with various cations were synthesized by the method shown in Scheme 1. A flask was charged with 20 mL of either 1*M* DABCO in DMF, DMP (pure), MPY (pure), PYR (pure and 50 vol % in DMF), or 1*M* TMP in toluene and purged with dry nitrogen for 20 min. Nafion 111P (80 mg) was then added to the flask and reacted for a total of 72 h at room temperature. For DABCO, DMP, and PYR, the reaction was performed under active nitrogen purge for 3 h and then sealed under a nitrogen environment for 69 h (72 h total). MPY and TMP were sealed under a nitrogen environment for 72 h with no active purge. Nafion 111P (80 mg) was also added to a TMA solution (45 wt % in water, 20 mL) without nitrogen purge. The swollen reacted membranes in the fluoride ion form were rinsed in fresh DI water three times more than ~3 h. Membranes reacted with TMP/toluene were washed first with DMF (50 mL) for 30 min before washing with fresh DI water three times over ~3 h. The membranes were then ion exchanged to the hydroxide ion form in 1*M* KOH (aq) solution for 3 h. The hydroxide exchange membranes were then removed from the solution and were rinsed in fresh DI water many times over ~24 h. The hydroxide ion form AEMs were then stored in DI water until further use. All AEMs synthesized in this study with the Nafion precursor are listed in Table I.

IEC and Water Sorption

The ion exchange capacities [IECs (meq g^{-1})] of the AEMs were determined using a Warder back titration. Approximately 20 mg of membrane (ca. 2 cm^2) was soaked in 3 mL of 0.06*M* KCl aqueous solution (~10 times excess moles of Cl^- assuming 100% conversion of —SO_2F to anion exchange sites) for at least 12 h. The membrane and KCl solution were then placed in an ice bath and titrated with 8.5 μ*M* HCl. Titration curves (pH) were recorded using an Accumet Excel dual channel pH meter (XL50, Fisher Scientific). The endpoint for titration was chosen based on the expected counter ion group, pH = 11.34 (KOH), 8.31 (K_2CO_3), and 4.03 ($KHCO_3$), respectively.

Water sorption (uptake) was measured on membranes weighing ~5 mg (ca. 1 cm^2). After membranes were immersed in DI

Table I. Nafion-Based AEMs Synthesized

AEM name	Reactant	Covalently attached cation
N-DABCO	1,4-Diazabicyclo [2.2.2]octane	Quaternized DABCO
N-DMP	1,4-Dimethylpiperazine	Piperazinium
N-MPY	1-Methylpyrrolidine	Pyrrolidinium
N-PYR	Pyridine	Pyridinium
N-TMA	Trimethylamine	Trimethylammonium
N-TMP	Trimethylphosphine	Trimethylphosphonium

water for 24 h, they were removed from the water, carefully patted dry to remove residual surface water and immediately weighed. The membranes were then dried at ambient room conditions and dry weights were then measured. Weights were recorded with a Precisa balance (XR 1253M-FR) with 0.01 mg accuracy. The percent of water uptake was calculated on a dry basis by:

$$\text{wt }\% = \frac{m_{\text{wet}} - m_{\text{dry}}}{m_{\text{dry}}} \times 100 \quad (1)$$

where m_{dry} and m_{wet} are the dry and wet mass of the membrane, respectively. A minimum of three experiments were conducted on each sample and the values reported are the average and standard deviation of those experiments. The hydration number, λ, for the membranes was also reported and calculated using the molecular weight of water $[M_w(H_2O)]$ and the measured IEC and water uptake of the membranes:

$$\lambda = \left(\frac{\text{wt }\%}{100}\right)\left(\frac{1000}{\text{IEC } M_w(H_2O)}\right) \quad (2)$$

Instruments

Infrared spectra were collected on a Fourier transform infrared spectrometer (Nicolet 6700 Series, Thermo Electron) equipped with both a single-reflection diamond attenuated total reflectance (ATR) crystal (Golden Gate™, Specac) and a sample holder (13 mm, ID, Specac) for transmission. The ATR has a ~0.5 mm^2 sampling area, where a consistent reproducible

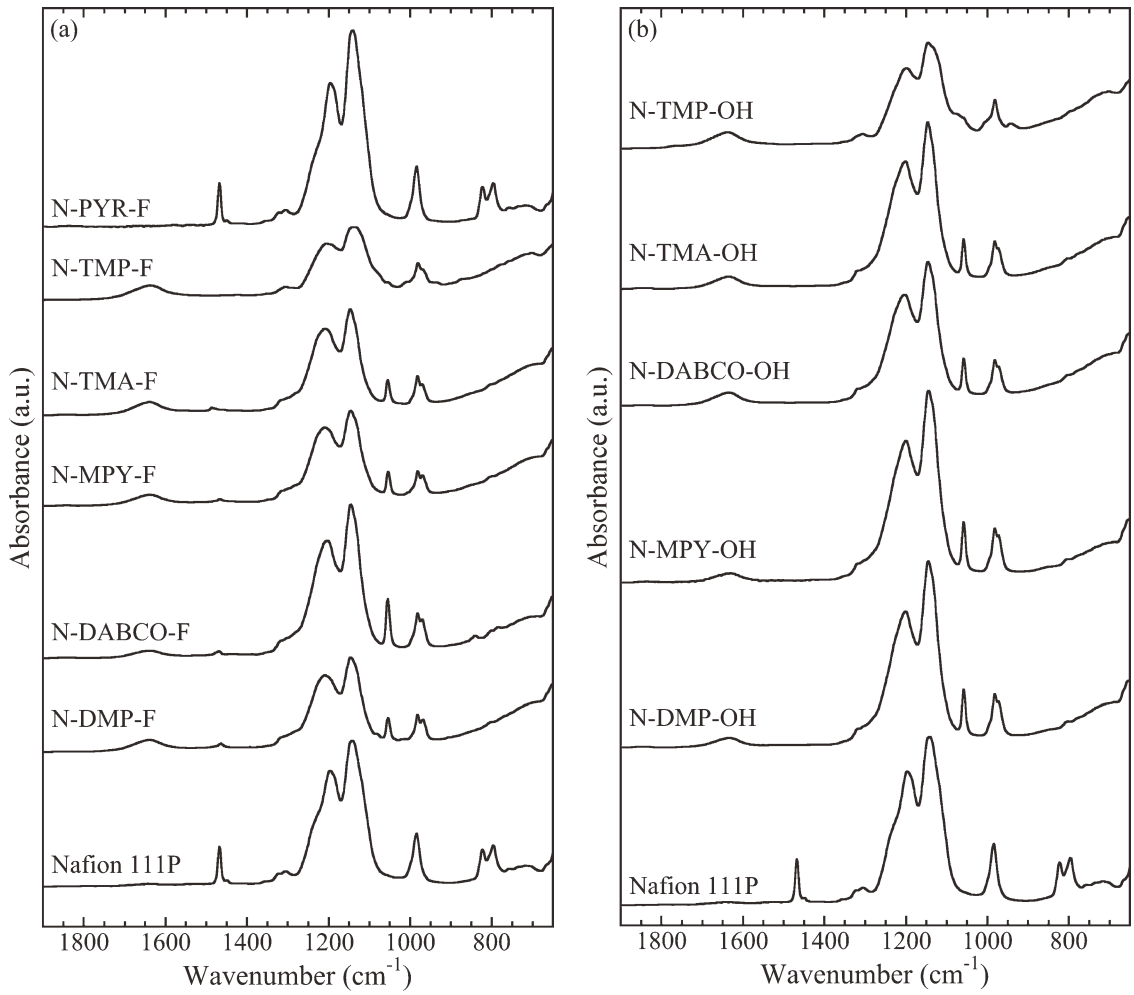

Figure 1. ATR infrared spectra of Nafion precursor (Nafion 111P), *N*-DMP, *N*-DABCO, *N*-MPY, *N*-TMA, *N*-TMP, and *N*-PYR in both the (a) fluoride and (b) hydroxide ion forms. Only infrared spectra ranging from 650 to 1900 cm^{-1} are shown to highlight specific key chemical bond vibrations in the polymer. Spectra are offset for clarity.

Applied Polymer SCIENCE

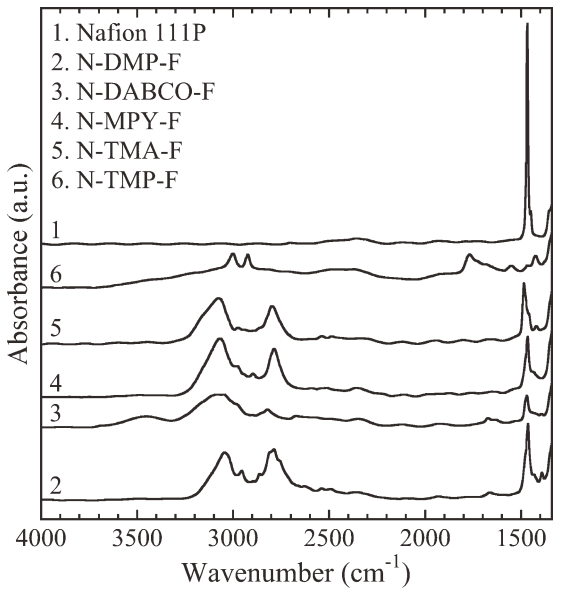

Figure 2. Infrared spectra (transmission) of Nafion 111P, *N*-DMP-F, *N*-DABCO-F, *N*-MPY-F, *N*-TMA-F, and *N*-TMP-F. Infrared spectra ranging from 1340 to 4000 cm^{-1} are shown to highlight specific areas of interest. Spectra are offset for clarity.

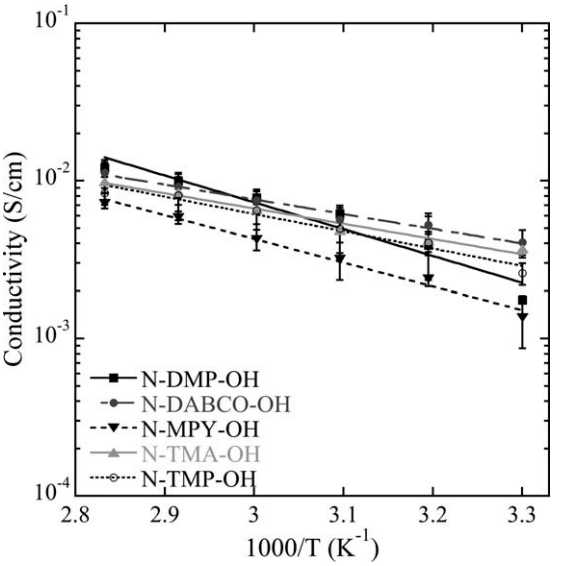

Figure 3. In-plane ionic conductivity as a function of temperature at 90% RH for *N*-DMP-OH, *N*-DABCO-OH, *N*-MPY-OH, *N*-TMA-OH, and *N*-TMP-OH.

pressure was applied to every sample. Infrared spectra were collected at a resolution of 4, 1.928 cm^{-1} data spacing, and 32 scans with an aperture of 25 and 10 for ATR and transmission experiments, respectively. Thermal stabilities were measured with thermogravimetric analysis (TGA; TA Instruments, Q50). Membrane samples were loaded on platinum pans and heated at 10°C min^{-1} under 10 mL min^{-1} nitrogen flow.

Ionic conductivity of polymer membranes was measured both through-the-plane (through-plane or transverse) and in-the-plane (in-plane or parallel) of the membrane between 10 Hz and 1 MHz with a Solartron AC impedance spectrometer (1260 impedance analyzer, 1287 electrochemical interface, Zplot software). Membranes (~25 μm in thickness) were hydrated with DI water for at least 24 h before conductivity measurements. Saturated membranes were then cut into squares (2 × 2 cm^2) for through-plane measurements or into strips (3 × 0.5 cm^2) for in-plane measurements and then loaded in hydrated form into the appropriate custom-made cells. Through-plane conductivity was measured using a two-electrode cell, consisting of 1.22 cm^2 stainless steel blocking electrodes within a custom-made Teflon cell. The prehydrated membranes were quickly enclosed within the Teflon cell to maintain hydration during the impedance measurement. Through-plane measurements were performed at room temperature, and the reported values are an average of three measurements. In-plane conductivity was measured using an open Teflon-coated stainless steel cell consisting of four parallel electrodes. The in-plane cell was placed in an environmental chamber (Tenney) with controlled temperature (ranging from 30 to 80°C) and humidity (90% RH). Alternating current was applied to the outer electrodes and impedance was measured between the inner two electrodes. The membranes were equilibrated at each temperature for 2 h and then six measurements were taken every subsequent 15 min. The reported conductivity was calculated from the average resistances of these steady state values at each temperature for at least two experiments per AEM. For both geometries, the real impedance was calculated from the *x*-intercept of the imaginary versus real impedance data over a high frequency range. Conductivity,

Table II. Ionic Conductivities (at 90% RH), Arrhenius Activation Energies, and Liquid Water Equilibrium Sorption for Nafion-Based AEMs in Hydroxide Ion Form

	Conductivity (mS cm^{-1})					
Membrane	30°C	80°C	E_A (kJ mol^{-1})	Water uptake (wt %)	IEC (meq g^{-1})	λ (mol H_2O/mol X[a])
N-DABCO-OH	4.1 ± 0.8	11.2 ± 2	17.9	18 ± 5	0.11 ± 0.04	99 ± 36
N-DMP-OH	1.76 ± 0.07	12.0 ± 2	32.6	10 ± 2	0.09 ± 0.03	70 ± 25
N-MPY-OH	1.4 ± 0.4	7.2 ± 0.2	28.8	8 ± 1	0.09 ± 0.02	48 ± 11
N-TMA-OH	3.7 ± 0.3	9.8 ± 3	18.5	19 ± 2	0.13 ± 0.01	77 ± 7
N-TMP-OH	2.6 ± 0.4	8.36 ± 0.04	21.0	10 ± 3	0.12 ± 0.01	45 ± 4

[a] X = covalently attached ionic group (i.e., $-SO_2X^+$).

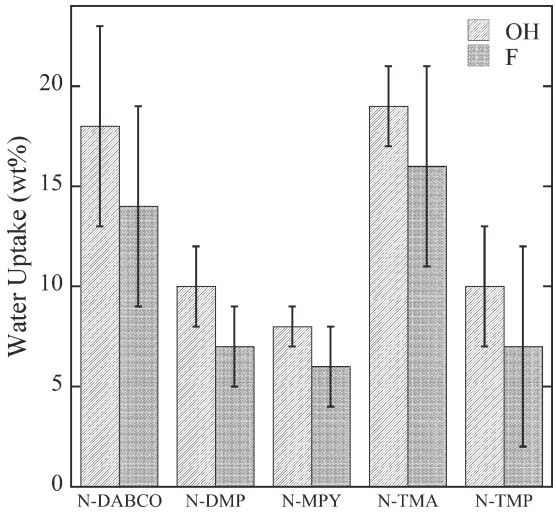

Figure 4. Water uptake for *N*-DABCO, *N*-DMP, *N*-MPY, *N*-TMA, and *N*-TMP in both the fluoride and hydroxide ion forms.

σ (S cm^{-1}), was calculated with the equation $\sigma = L/(AR)$, where L is the distance between electrodes and A is the cross-sectional area of ion conduction and R is the real impedance or resistance. More details concerning the conductivity apparatus and procedures can be found elsewhere.[57–59]

AEM Stability

To further test the stability of AEMs prepared with different cationic groups, the AEMs were tested under six different conditions for 24 h: hydrated at room temperature (i.e., never dried), dried at room temperature, dried under vacuum at 80°C, heated in water at 80°C, immersed in 1*M* KOH at room temperature, and refluxed in 1*M* KOH at 80°C. Through-plane ionic conductivity of the hydrated membranes and TGA of the dried membranes were performed to provide a qualitative measure of chemical degradation of the AEMs after exposure to these six conditions. AEMs that were exposed to KOH were washed several times with fresh DI water for 24 h after exposure to terminate additional degradation and remove excess KOH. Dry membranes were rehydrated for conductivity measurements and wet membranes were dried at room conditions for TGA.

RESULTS AND DISCUSSION

Figure 1 shows the ATR infrared spectra of the Nafion precursor (Nafion 111P) and Nafion-based AEMs with various cations in both the fluoride and hydroxide ion forms. Three distinct bands, 1468, 823, and 796 cm^{-1}, are present in Nafion precursor and are associated with the sulfonyl fluoride pendant group (—SO_2F). The band at 1468 cm^{-1} represents the asymmetric stretch of the O=S=O in the sulfonyl fluoride pendant group (—SO_2F), whereas the doublet at 823 and 796 cm^{-1} is associated with the S—F stretching vibrations of this pendant group.[53,60] The bands that are associated with the sulfonyl fluoride pendant group are not present in the fluoride or hydroxide ion forms of five of the Nafion AEMs that were synthesized (*N*-DMP, *N*-DABCO, *N*-MPY, *N*-TMA, and *N*-TMP) indicating a reaction with the sulfonyl fluoride producing a covalently bound cation. However, the bands associated with the —SO_2F pendant group are still present in *N*-PYR-F indicating that no reaction occurred between PYR and sulfonyl fluoride.

The fluoride and hydroxide ion forms of *N*-DMP, *N*-DABCO, *N*-MPY, *N*-TMA, and *N*-TMP all have bands between 1016 and 1059 cm^{-1} that are not present in the Nafion precursor. For *N*-DMP, *N*-DABCO, *N*-MPY, and *N*-TMA, this band can be assigned to the symmetric stretch of O=S=O in the $SO_2N^+R_3$ pendent group.[56] This band may also be associated with ring vibrations, such as deformation and CH_2 twist of the cyclic pendent groups in *N*-DMP,[61,62] *N*-DABCO,[63] and *N*-MPY.[64] This band shifts to lower wave numbers, 1016–1017 cm^{-1}, in the phosphonium cation AEM, *N*-TMP and is associated with the symmetric stretch of O=S=O in the $SO_2P^+R_3$ pendent group.

The one band in the Nafion precursor at 984 cm^{-1}, which represents the asymmetric stretch of the C—O—C in the side chain, becomes two distinct bands in the fluoride ion forms of *N*-DMP, *N*-DABCO, *N*-MPY, and *N*-TMA, and a shoulder in the hydroxide ion forms. These two bands at 967–969 cm^{-1} and 981–982 cm^{-1} have been reported to represent the symmetric and asymmetric stretching vibration of C—O—C, respectively.[65] This band in the phosphonium AEM, *N*-TMP, shifts to lower wave numbers, 937–940 cm^{-1}. We suggest that the symmetric vibration becomes undampened in the ionic forms. The band at 967–969 cm^{-1} may also be associated with C—H and ring vibrations of the cationic groups in the AEMs.[25,34,61,63,64] The two large infrared bands at 1134–1143 and 1196–1208 cm^{-1} represent the symmetric and asymmetric C—F_2 stretch, respectively.[53,66]

Figure 2 shows the transmission infrared spectra for *N*-DMP-F, *N*-DABCO-F, *N*-MPY-F, *N*-TMA-F, and *N*-TMP-F compared to Nafion precursor. In this study, the infrared band at 1468 cm^{-1} associated with the asymmetric stretching of the O=S=O bonds in the sulfonyl fluoride (—SO_2F) pendent group in the Nafion precursor decreased in intensity on conversion to AEMs. However, notice how the band is still present in the transmission infrared spectra for all AEMs, just lower in intensity. Among the AEMs synthesized, the relative intensity of the 1468 cm^{-1} band differs when comparing ATR and transmission infrared spectra. The complete disappearance in ATR compared with only a decrease in intensity in transmission suggests that the sulfonyl fluoride pendent groups react completely near the surface of the membrane but not uniformly throughout the thickness of the membrane. Greso et al.[53] reported a similar increase in sulfonyl fluoride pendent group concentration with increasing distance from the membrane surface when reacting primary amines within the Nafion precursor membrane. The observance of partially reacted sulfonyl fluoride pendent groups via transmission infrared spectra is also consistent with the IEC results summarized in Table II.

Figure 2 also shows the appearance of several infrared bands in the region of 2700–3100 cm^{-1} in the AEMs that are absent in the Nafion precursor. The two main bands located at 3045 and 2788 cm^{-1} in *N*-DMP-F are associated with the CH_2 and CH_3 stretching vibrations of the dimethylpiperazinium ring in *N*-DMP-F.[61,62] Similarly bands associated with CH_2 stretching also

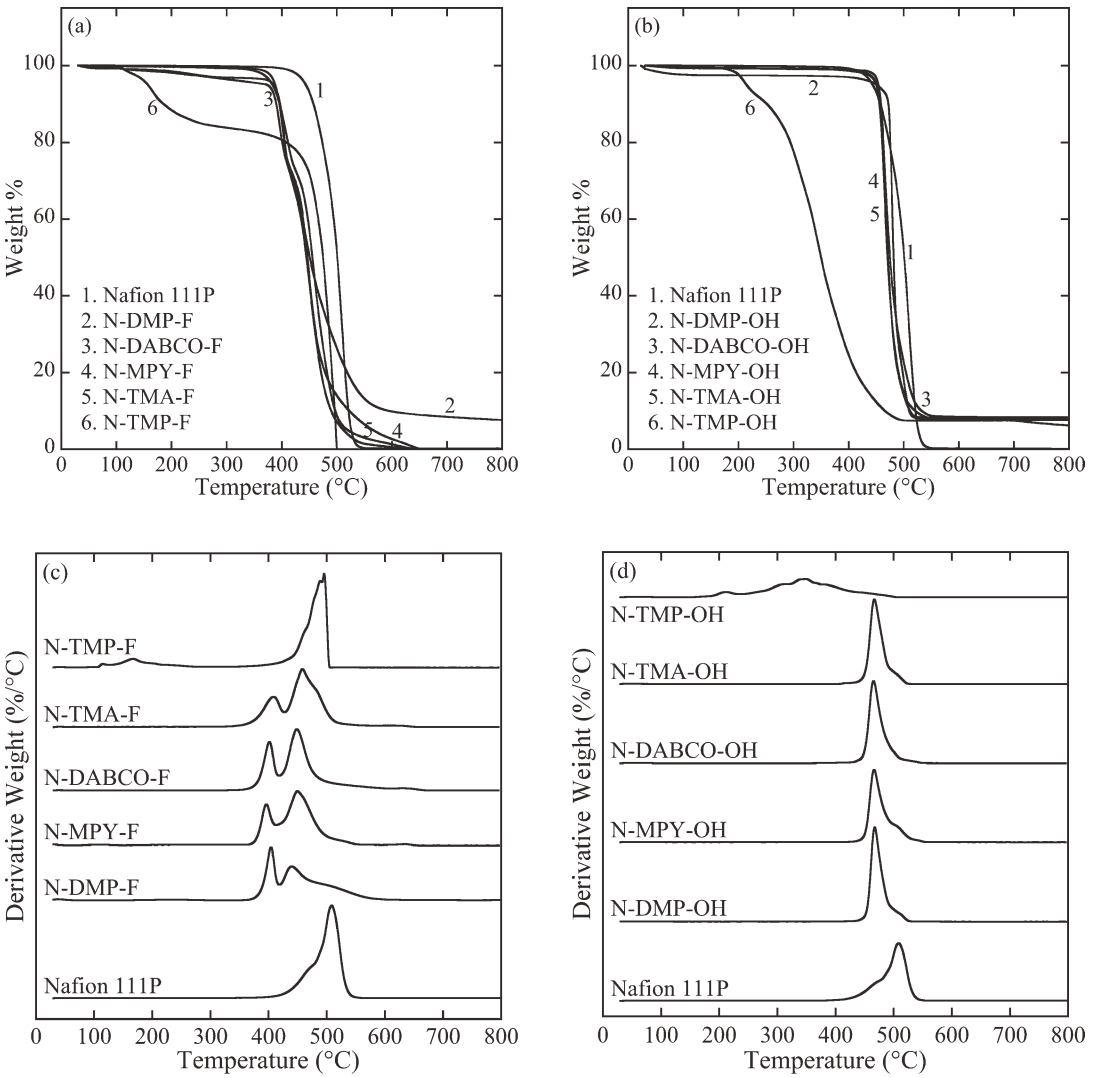

Figure 5. Thermal gravimetric analysis of Nafion 111P, *N*-DMP, *N*-DABCO, *N*-MPY, *N*-TMA, and *N*-TMP: weight loss and derivative weight loss of (a, c) fluoride and (b, d) hydroxide ion forms, respectively.

appear at 3049–3084 cm^{-1} in *N*-DABCO-F[63,67] and 2787 and 3069 cm^{-1} in *N*-MPY-F.[64] In *N*-TMA-F, two bands appear that can be associated with CH_3 vibrations, 2797 and 3076 cm^{-1}.[14,18] In *N*-TMP-F, the appearance of two additional bands is noticed that are associated with CH_3 vibrations, 2924 and 3001 cm^{-1}.[68,69] The appearance of the bands associated with CH_2 and CH_3 modes further confirms the successful partial conversion of the Nafion precursor to AEMs with covalently attached cation groups.

Figure 3 shows the hydroxide conductivities of the AEMs in this study. The hydroxide conductivities of the various cations are all within a similar range: 1.4–4.1 mS cm^{-1} at 30°C and 8.36–12.0 mS cm^{-1} at 80°C. The Arrhenius activation energies range between 17.9 and 32.6 kJ mol^{-1}. It is important to note that while the AEMs were exchanged with 1*M* KOH to the hydroxide form before the conductivity measurements, no care was taken to limit the AEMs exposure to air. As a result, the AEMs may undergo an ion exchange or carbonation to a carbonate (CO_3^{2-}) or bicarbonate (HCO_3^-) ion form due to exposure to CO_2 in ambient air. Yan and Hickner[17] recently demonstrated that the hydroxide ion conductivity of an AEM decreases over a period of 3–4 days and asymptotically approaches the conductivity of a bicarbonate exchanged AEM, ~fourfold lower than the original hydroxide ion conductivity. Yanagi and Fukuta[70] have shown that the concentration of hydroxide within an AEM is reduced to near 0% after the first 30 min of exposure to air replaced with a combination of CO_3^{2-} and HCO_3^-. In this study, the conductivity experiments from 30 to 80°C were conducted in humid air (90% RH) over a period of 20 h. The AEMs exposure to atmospheric carbon dioxide was not limited throughout the conductivity measurement or the prior ion exchange procedure (>24 h), making it reasonable to assume that the AEMs may have converted to the bicarbonate form. However, the rate of carbonation is unknown as this can be highly dependent on the cation type, polymer chemistry, polymer morphology, and membrane water content. Compared with the conductivities reported in our study, Yan and Hickner[17] also

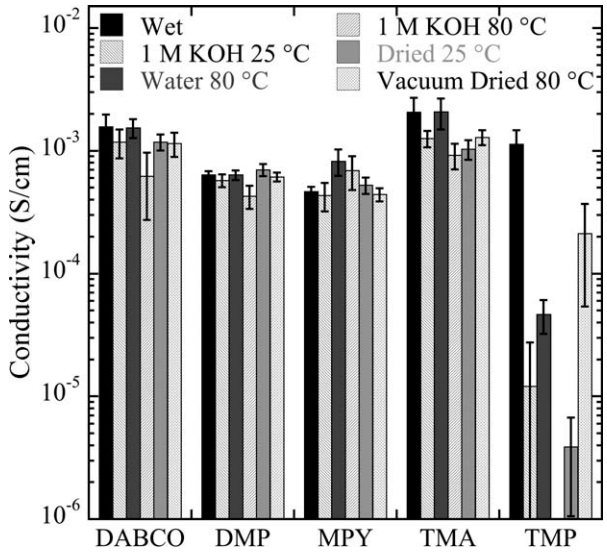

Figure 6. Chemical stability measured by through-plane ionic conductivity of hydrated AEMs after exposure to various conditions for 24 h.

reported similar bicarbonate ion conductivities of TMA quaternized polysulfone-based AEMs (6.5–27 mS cm^{-1}). Although Faraj et al.[43] have reported similar bicarbonate ion conductivities for styrene-butadiene-styrene-based AEMs with quaternized DABCO cations (3.2–9.2 mS cm^{-1}, 30°C). Other investigators have also reported similar hydroxide ion conductivities in air for AEMs with guanidinium cations (5 mS cm^{-1}, 20°C, 0.86 meq g^{-1})[71] and TMA cations (1.6–29 mS cm^{-1}, 20–30°C, 0.06–1.63 meq g^{-1}).[13,14,16,18,20,21] Arges et al.[40] reported similar hydroxide conductivities for phosphonium-functionalized polysulfone when exposed to air (10–12.5 mS cm^{-1}).

Adams et al.[5] have reported that the AEM AFC is a self-cleaning system. In other words, the carbonated AEM will exchange to the hydroxide ion form during fuel cell operation, reaching a new equilibrium in the hydroxide ion rich environment. Others have reported the evolution of carbon dioxide in the fuel cell exhaust during start up confirming this ion exchange of the AEM from bicarbonate to hydroxide ion form during AFC operation.[70,72,73] If this ion exchange of the AEM within an AFC is a universal phenomena, then an increase in conductivity of up to fourfold could be expected.

Figure 4 shows the equilibrium water uptake of the hydroxide and fluoride ion forms of *N*-DABCO, *N*-DMP, *N*-MPY, *N*-TMA, and *N*-TMP. For each AEM, water uptakes of the hydroxide and fluoride ion forms are similar within experimental error. The TMA and DABCO AEMs have the highest water uptake at 19 and 18 wt %, respectively. Although the TMP, MPY, and DMP AEMs have lower water uptakes of 10, 8, and 10 wt %, respectively. Several groups have reported water uptakes for AEMs in this range.[13,16,19,20,71] The AEM water uptake is an important property to optimize. If the AEM absorbs too much water, the membrane can become mechanically weak but if not enough water is present this usually leads to low water-dependent ionic conductivities. The water uptake for the AEMs studied here are lower than that of Nafion proton exchange membranes (33–40%),[56] but it is clear from the conductivities reported in Figure 3 that it is sufficient for good ionic conductivity for IECs as low as ~0.1 meq g^{-1} (Table II).

A summary of conductivities, activation energies, IECs, water uptake, and hydration numbers (λ) for all the membranes investigated are listed in Table II. IEC was measured by Warder titration, which can distinguish between the presence of hydroxide, carbonate, and bicarbonate ions based on the pH of the starting solution and endpoint. After several days of exposure to ambient air, the starting and ending pH values confirmed that all alkaline AEMs in this study had in fact converted completely to the bicarbonate form (HCO_3^-). The IECs for these AEMs range from 0.09 to 0.13 meq g^{-1}. The Nafion precursor has a sulfonyl fluoride functionality of 0.9 meq g^{-1}, suggesting that

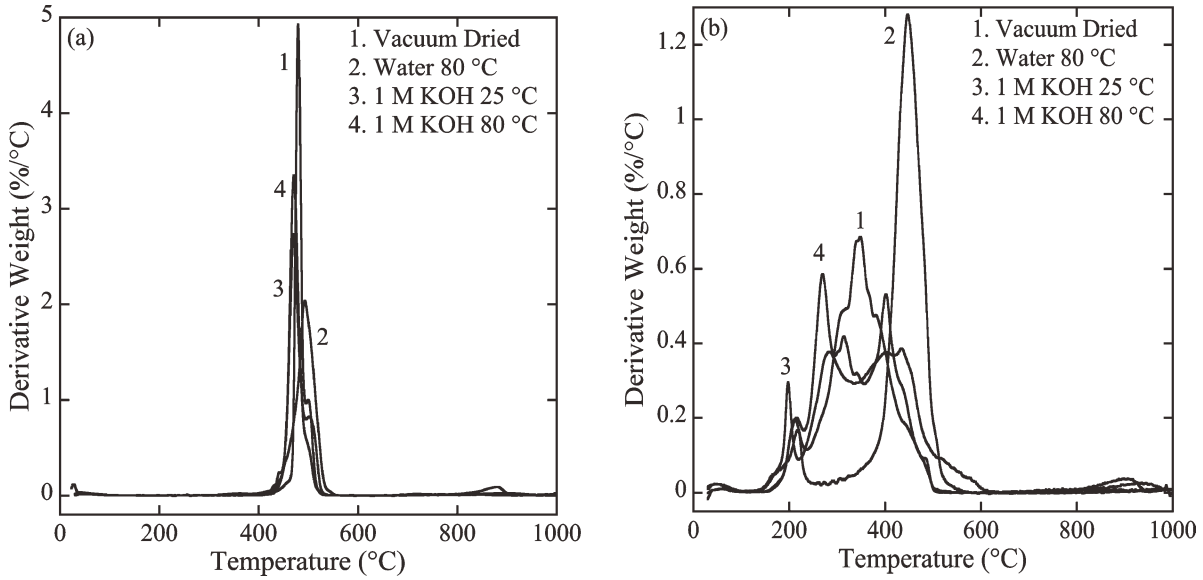

Figure 7. Thermal stability (derivative weight loss) of (a) *N*-DMP-OH and (b) *N*-TMP-OH after exposure to various conditions for 24 h.

only a partial functionalization was achieved (i.e., partial conversion of the $-SO_2F$ to $-SO_2X^+$). This corroborates with the transmission infrared spectra results (Figure 2) showing only a lower intensity and not a complete disappearance of the 1468 cm^{-1} band associated with the sulfonyl fluoride group. Even though the IECs of the AEMs in this study are 7–10-fold lower than the acid form of Nafion ($-SO_3^-H^+$), the hydration numbers, 46–99 mol H_2O/mol X^+, for these AEMs are higher than Nafion (21 mol H_2O/mol SO_2^-).

Figure 5 shows the thermal stability of the AEMs in this study compared to the Nafion precursor. Each membrane was dried under vacuum at room temperature for 12 h before TGA experiments. The Nafion precursor degrades in a single step with a 508°C derivative peak maximum. The thermal stability of *N*-TMP is significantly different than the Nafion precursor and the other AEMs. *N*-TMP exhibits derivative peak maximums at 167 and 211°C for the fluoride and hydroxide ion forms, respectively. In the fluoride form, the data suggest that the cation is cleaved and initiates side chain degradation at a lower temperature with ~20 wt % loss before 500°C. In the hydroxide form, the data suggest that a thermally liable cation initiates thermal degradation of the entire polymer around 200°C. The other AEMs appear to be more thermally stable with onsets of degradation greater than 300°C and 400°C in the fluoride ion and hydroxide ion forms, respectively. Trostyanskaya and Makarova[7] have also reported that phosphoniums have a lower thermal stability than ammoniums. The introduction of covalently attached cations does, however, change the thermal properties as compared with the Nafion precursor as evidenced by the derivative plots.

The chemical stability of the AEMs was studied by exposing them to different environments such as dehydration, high pH, and elevated temperature. Chemical stability was measured by conductivity (Figure 6) and TGA (Figure 7) of the AEMs after exposures to these environments. Figure 6 shows that the ionic conductivities of *N*-DABCO-OH, *N*-DMP-OH, *N*-MPY-OH, and *N*-TMA-OH are not significantly affected when exposed to high temperature (water saturated, 80°C), dehydration (under vacuum, 80°C), or high pH (1*M* KOH, 80°C). However, significantly lower conductivities were observed for *N*-TMP after exposure to all the chosen conditions. The most extreme case was at 1*M* KOH at 80°C, where the membrane lost mechanical strength and broke apart into fragments that were too small to measure conductivity. Note that the through-plane conductivities in Figure 6 are slightly lower than the in-plane conductivities reported in Figure 3 as one would expect due to differences in measurement conditions (fully saturated for through-plane compared to 90% RH for in-plane experiments) and additional interfacial resistance in through-plane experiments at low overall membrane resistances.

These conductivity results are further confirmed by the TGA results shown in Figure 7. In this figure, *N*-DMP-OH was compared with *N*-TMP-OH. The TGA results of the other AEMs, *N*-DABCO-OH, *N*-MPY-OH, and *N*-TMA-OH are not shown here, but the results were similar to *N*-DMP-OH. The TGA results of *N*-DMP-OH after exposure to all chosen conditions are similar with onsets of degradation above 400°C and derivative peak maxima between 467 and 493°C, implying good chemical stability of *N*-DMP-OH. The TGA results of *N*-TMP-OH after exposure to all chosen conditions, however, are not similar. After exposure to several of the conditions, the derivative peaks become bimodal. This could imply that the chemical degradation that occurs under different conditions affects the thermal degradation mechanism of *N*-TMP-OH. Overall, the thermal degradation temperatures for these membranes are higher than expected suggesting other mechanisms may occur and therefore warrants further investigation.

CONCLUSIONS

In this work, the synthesis of Nafion-based AEMs with trimethylammonium, trimethylphosphonium, piperazinium, pyrrolidinium, pyridinium, and quaternized DABCO as the covalently attached cations was investigated. Infrared spectroscopy verified the partial functionalization of precursor Nafion with all cations except pyridinium and showed that the cation concentration varied as a function of membrane thickness. The conductivity, water uptakes, and IECs were found to be similar for all Nafion AEMs and sufficiently high. The effects of hydration levels, temperature, and pH on the stability of AEMs with different cation types were investigated. High chemical and thermal stability was observed for all AEMs with the exception of the trimethylphosphonium cation AEM, which demonstrated decreased performance for all conditions studied. The high thermal and chemical stability of trimethylammonium, piperazinium, pyridinium, and quaternized DABCO Nafion-based AEMs make them promising candidates as polymer electrolytes for solid-state AFCs.

ACKNOWLEDGMENTS

This work was supported by the U.S. Army Research Laboratory Materials Center of Excellence, under grant number W911NF-06-2-0013.

REFERENCES

1. Varcoe, J. R.; Slade R. C. *T. Fuel Cells* **2005,** *5*, 187.
2. Hibbs, M. R.; Fujimoto, C. H.; Cornelius, C. J. *Macromolecules* **2009,** *42*, 8316.
3. Chempath, S.; Einsla, B. R.; Pratt, L. R.; Macomber, C. S.; Boncella, J. M.; Rau, J. A.; Pivovar, B. S. *J. Phys. Chem. C* **2008,** *112*, 3179.
4. Lu, S. F.; Pan, J.; Huang, A. B.; Zhuang, L.; Lu, J. T. *Proc. Natl. Acad. Sci. USA* **2008,** *105*, 20611.
5. Adams, L. A.; Poynton, S. D.; Tamain, C.; Slade, R. C. T.; Varcoe, J. R. *ChemSusChem* **2008,** *1*, 79.
6. Merle, G.; Wessling, M.; Nijmeijer, K. *J. Membr. Sci.* **2011,** *377*, 1.
7. Trostyanskaya E. B.; Makarova, S. B. *Zh. Prikl. Khim.* **1966,** *39*, 1754.
8. Bauer, B.; Strathmann, H.; Effenberger, F. *Desalination* **1990,** *79*, 125.
9. Sata, T.; Teshima, K.; Yamaguchi, T. *J. Polym. Sci. Part A: Polym. Chem.* **1996,** *34*, 1475.

10. Sata, T.; Tsujimoto, M.; Yamaguchi, T.; Matsusaki, K. *J. Membr. Sci.* **1996,** *112*, 161.
11. Wang, J.; He, R.; Che, Q. J. *Colloid Interface Sci.* **2011,** *361*, 219.
12. Zhang, F.; Zhang, H.; Qu, C.; Ren, J. *J. Power Sources* **2011,** *196*, 3099.
13. Zhao, Z.; Wang, J.; Li, S.; Zhang, S. *J. Power Sources* **2011,** *196*, 4445.
14. Xu, H. K.; Fang, J.; Guo, M. L.; Lu, X. H.; Wei, X. L.; Tu, S. *J. Membr. Sci.* **2010,** *354*, 206.
15. Zhang, H. W.; Zhou, Z. T. *J. Appl. Polym. Sci.* **2008,** *110*, 1756.
16. Xiong, Y.; Liu, Q. L.; Zeng, Q. H. *J. Power Sources* **2009,** *193*, 541.
17. Yan, J. L.; Hickner, M. A. *Macromolecules* **2010,** *43*, 2349.
18. Zhou, J. F.; Unlu, M.; Anestis-Richard, I.; Kohl, P. A. *J. Membr. Sci.* **2010,** *350*, 286.
19. Park, J. S.; Park, S. H.; Yim, S. D.; Yoon, Y. G.; Lee, W. Y.; Kim, C. S. *J. Power Sources* **2008,** *178*, 620.
20. Luo, Y. T.; Guo, J. C.; Wang, C. S.; Chu, D. J. *Power Sources* **2010,** *195*, 3765.
21. Slade, R. C. T.; Varcoe, J. R. *Solid State Ionics* **2005,** *176*, 585.
22. Varcoe, J. R.; Slade, R. C. T.; Yee, E. L. H.; Poynton, S. D.; Driscoll, D. J.; Apperley, D. C. *Chem. Mater.* **2007,** *19*, 2686.
23. Varcoe, J. R.; Slade, R. C. T.; Wright, G. L.; Chen, Y. L. *J. Phys. Chem. B* **2006,** *110*, 21041.
24. Varcoe, J. R. *Phys. Chem. Chem. Phys.* **2007,** *9*, 1479.
25. Xiong, Y.; Fang, J.; Zeng, Q. H.; Liu, Q. L. *J. Membr. Sci.* **2008,** *311*, 319.
26. Clark, T. J.; Robertson, N. J.; Kostalik, H. A., IV; Lobkovsky, E. B.; Mutolo, P. F.; Abruña, H. D.; Coates, G. W. *J. Am. Chem. Soc.* **2009,** *131*, 12888.
27. Hibbs, M. R.; Hickner, M. A.; Alam, T. M.; McIntyre, S. K.; Fujimoto, C. H.; Cornelius, C. J. *Chem. Mater.* **2008,** *20*, 2566.
28. Kostalik, H. A.; Clark, T. J.; Robertson, N. J.; Mutolo, P. F.; Longo, J. M.; Abruña, H. D.; Coates, G. W. *Macromolecules* **2010,** *43*, 7147.
29. Stevens, T. S.; Creighton, E. M.; Gordon, A. B.; MacNicol, M. *J. Chem. Soc.* **1928**, 3193.
30. Sommelet, M. *Comptes Rendus* **1937,** *205*, 56.
31. Macomber, C. S.; Boncella, J. M.; Pivovar, B. S.; Rau, J. A. *J. Therm. Anal. Calorim.* **2008,** *93*, 225.
32. Ye, Y.; Elabd, Y. A. Chemical Stability of Anion Exchange Membranes for Alkaline Fuel Cells. In Polymers for Energy Storage and Delivery: Polyelectrolytes for Batteries and Fuel Cells. Page, K.A.; Soles, C.L.; Runt, J., Eds. Oxford University Press, ACS Symposium Series, in press.
33. Li, Y.; Xu, T.; Gong, M. *J. Membr. Sci.* **2006,** *279*, 200.
34. Li, Y.; Xu, T. W. *J. Appl. Polym. Sci.* **2009,** *114*, 3016.
35. Yao, W.; Tsai, T.; Chang Y.-M.; Chen, M. US Patent 6,183,914, 2001.
36. Brylev, O.; Alloin, F.; Duclot, M.; Souquet, J. L.; Sanchez, J. Y. *Electrochim. Acta* **2003,** *48*, 1953.
37. Stokes, K. K.; Orlicki, J. A.; Beyer, F. L. *Polym. Chem.* **2011,** *2*, 80.
38. Gu, S.; Cai, R.; Luo, T.; Chen, Z.; Sun, M.; Liu, Y.; He, G.; Yan, Y. *Angew. Chem. Int. Ed.* **2009,** *48*, 6499.
39. Tomoi, M.; Ogawa, E.; Hosokawa, Y.; Kakiuchi, H. J. *Polym. Sci. Polym. Chem. Ed.* **1982,** *20*, 3015.
40. Arges, C. G.;Kulkarni, S.; Baranek, A.; Pan, K. -J.; Jung, M. -S.; Patton, D.; Mauritz, K. A.; Ramani, V. *ECS Trans.* **2010,** *33*, 1903.
41. Jovanovski, V.; Marcilla, R.; Mecerreyes, D. *Macromol. Rapid Commun.* **2010,** *31*, 1646.
42. Pont, A.-L.; Marcilla, R.; De Meatza, I.; Grande, H.; Mecerreyes, D. J. *Power Sources* **2009,** *188*, 558.
43. Faraj, M.; Elia, E.; Boccia, M.; Filpi, A.; Pucci, A.; Ciardelli, F. J. *Polym. Sci. Part A: Polym. Chem.* **2011,** *49*, 3437.
44. Pandey, A. K.;Goswami, A.; Sen, D.; Mazumder, S.; Childs, R. F. *J. Membr. Sci.* **2003,** *217*, 117.
45. Schmitt, F.; Granet, R.; Sarrazin, C.; Mackenzie, G.; Krausz, P. *Carbohydr. Polym.* **2011,** *86*, 362.
46. Scindia, Y. M.; Pandey, A. K.; Reddy, A. V. *R. J. Membr. Sci.* **2005,** *249*, 143.
47. Sollogoub, C.; Guinault, A.; Bonnebat, C.; Bennjima, M.; Akrour, L.; Fauvarque, J. F.; Ogier, L. *J. Membr. Sci.* **2009,** *335*, 37.
48. Stoica, D.; Alloin, F.; Marais, S.; Langevin, D.; Chappey, C.; Judeinstein, P. *J. Phys. Chem. B* **2008,** *112*, 12338.
49. Agel, E.; Bouet, J.; Fauvarque, J. F. *J. Power Sources* **2001,** *101*, 267.
50. Komkova, E. N.; Stamatialis, D. F.; Strathmann, H.; Wessling, M. *J. Membr. Sci.* **2004,** *244*, 25.
51. Robertson, N. J.; Kostalik, H. A.; Clark, T. J.; Mutolo, P. F.; Abruna, H. D.; Coates, G. W. *J. Am. Chem. Soc.* **2010,** *132*, 3400.
52. Vinodh, R.; Ilakkiya, A.; Elamathi, S.; Sangeetha, D. *Mater. Sci. Eng. B* **2010,** *167*, 43.
53. Greso, A. J.; Moore, R. B.; Cable, K. M.; Jarrett, W. L.; Mauritz, K. A. *Polymer* **1997,** *38*, 1345.
54. Grot, W. G. US Patent 4,030,988, 1977.
55. Kong, X.; Wadhwa, K.; Verkade, J. G.; K. Schmidt-Rohr. *Macromolecules* **2009,** *42*, 1659.
56. Salerno, H. L. S.; Beyer, F. L.; Elabd, Y. A. *J. Polym. Sci. Part B: Polym. Phys.* **2012,** *50*, 552.
57. Chen, H.; Choi, J. H.; Salas-de La Cruz, D.; Winey, K. I.; Elabd, Y. A. *Macromolecules* **2009,** *42*, 4809.
58. DeLuca, N. W.; Elabd, Y. A. *J. Membr. Sci.* **2006,** *282*, 217.
59. Elabd, Y. A.; Walker, C. W.; Beyer, F. L. *J. Membr. Sci.* **2004,** *231*, 181.
60. Swaminathan, P.; Disley, P. F.; Assender, H. E. *J. Membr. Sci.* **2004,** *234*, 131.
61. Dega-Szafran, Z.; Katrusiak, A.; Szafran, M. J. *Mol. Struct.* **2008,** *880*, 69.
62. Dega-Szafran, Z.; Katrusiak, A.; Szafran, M. J. *Mol. Struct.* **2008,** *887*, 92.

63. Barczynski, P.; Dega-Szafran, Z.; Katrusiak, A.; Perdoch, W.; Szafran, M. J. *Mol. Struct.* **2009,** *933*, 46.

64. Babushkina, O. B. Z. Naturforsch. A: *Phys. Sci.* **2008,** *63*, 66.

65. Heitner-Wirguin, C. *Polymer* **1979,** *20*, 371.

66. Laporta, M.; Pegoraro, M.; Zanderighi, L. *Phys. Chem. Chem. Phys.* **1999,** *1*, 4619.

67. Barczynski, P.; Dega-Szafran, Z.; Katrusiak, A.; Szafran, M. J. *Mol. Struct.* **2011,** *998*, 240.

68. Wojtas, M.; Medycki, W.; Baran, J.; Jakubas, R. *Chem. Phys.* **2010,** *371*, 66.

69. Minkwitz, R.; Medger, G.; Preut, H. Z. *Anorg. Allg. Chem.* **1992,** *614*, 102.

70. Yanagi, H.; Fukuta, K. *ECS Trans.* **2008,** *16*, 257.

71. Wang, J. H.; Li, S. H.; Zhang, S. B. *Macromolecules* **2010,** *43*, 3890.

72. Fukuta, K.; Inoue, H.; Watanabe, S.; Yanagi, H. *ECS Trans.* **2009,** *19*, 23.

73. Watanabe, S.; Fukuta, K.; Yanagi, H. *ECS Trans.* **2010,** *33*, 1837.